THE JOURNAL OF
PHYSICAL CHEMISTRY

VOLUME 80, NUMBER 7 MARCH 25, 1976

Diffusion Theory of Imprisonment of Atomic Resonance Radiation at Low Opacities

R. P. Blickensderfer, W. H. Breckenridge,*[1] and Jack Simons[2]

Department of Chemistry, University of Utah, Salt Lake City, Utah 84112 (Received October 20, 1975)

Publication costs assisted by the Petroleum Research Fund

The modified diffusion theory of imprisonment of atomic resonance radiation is shown to be valid in the low-opacity region, and is extended to include infinite slab, infinite cylinder, and spherical vessel geometries. Calculations are presented which allow the use of the theory for pure Doppler, pure Lorentz, and Voigt spectral line shapes.

I. Introduction

Experimental investigation of chemical and physical processes involving fluorescent electronically excited atoms is sometimes complicated by the troublesome phenomenon of radiation imprisonment.[3-13] Because of repeated emission and reabsorption of resonance quanta, the "effective" lifetime of an excited atomic state may depend both on the concentration of ground-state atoms and the geometry of the enclosing cell, often in a complicated fashion. With more sensitive detection techniques it is sometimes possible to conduct experiments at extremely low ground-state number densities, where the excited-state lifetime is increased negligibly. More commonly, however, the effects of radiation imprisonment can be reduced but not completely eliminated.[3,8-11,14] Obviously, certain practical optical devices such as lasers also have optimum operating conditions where imprisonment considerations cannot be ignored. A tractable theoretical model of the imprisonment process, which could be applied to experimentally convenient vessel geometries and low absorber opacities,[15] would be useful for determining limiting conditions of negligible imprisonment and for calculating small corrections to lifetimes when sufficiently low atom densities cannot be attained and direct measurements are difficult or impossible.[3,4,8-10]

In very high opacity situations, for infinite slab or infinite cylinder geometries, the "incoherent scattering" theory of Holstein has been quite successful in predicting apparent lifetimes of $Hg(^3P_1)$.[6,8,11,16] For the high opacity limit, simple analytical approximations are found to be adequate solutions of the Holstein integro-differential equations for radiative transfer.[6,7] Van Volkenburgh and Carrington,[5] using numerical analysis techniques, have extended the Holstein formulation for an infinite slab to Doppler line-shape systems of intermediate opacity.

For the low-opacity region of interest here, Michael and Yeh[8] have pointed out that the earliest treatment of radiation imprisonment (the infinite slab diffusion theory of Milne,[13,17] as modified by Samson[13,18]) will fit quite successfully the available $Hg(^3P_1)$ lifetime data if the width of the slab is identified with the radius of a cylindrical experimental vessel. The success of the Samson modification of the Milne theory rests on the use of a single "equivalent" [8,13] opacity to approximate the more complicated situation in which the scattered (imprisoned) radiation has a spectral distribution related to the absorption coefficient distribution of the ground-state atoms (e.g., for the common case of a pressure-broadened absorption line). Thus the photons are assumed to be incoherently rather than coherently scattered.

Holstein,[6] and Biberman,[19] have since shown that the transport equations for incoherently scattered resonance radiation (under Doppler- or dispersion-broadening conditions) cannot properly be solved by assuming the existence of an average absorption coefficient (i.e., a photon mean free path), so that a simple diffusion model is not expected to predict imprisonment lifetimes accurately. However, while it is certainly true that the Samson–Milne treatment is not successful in the very high opacity region of interest to Holstein and Biberman, there is good reason to believe that the simpler diffusion theory can provide an adequate model for low-opacity experimental situations for which the use of an average absorption coefficient, or equivalent opacity, is a less drastic approximation.

In this paper, we: (1) show that the use of an "equiva-

lent" opacity is valid in the limit of low absorber opacities, for a variety of line shapes, and therefore justify the use of the Samson–Milne diffusion theory as a very good approximation under such conditions; (2) extend the radiation diffusion theory to the geometries of sphere and of infinite cylinder, which may be better approximations to certain experimental vessels than the infinite slab; and (3) calculate equivalent opacities in the low-opacity regime for the following line shapes: (i) pure Doppler broadening, (ii) pure Lorentz (pressure) broadening, and (iii) Voigt broadening (Doppler, Lorentz, and Heisenberg (natural) broadening).

II. The Diffusion Model

We first treat an idealized two-level atomic system in a cell under the influence of a weak external source of resonance radiation. The system has a concentration (n) of ground-state atoms of a certain element and a concentration (n^*) of atoms in a particular excited state, with $n^* \ll n$. The absorption coefficient for ground-state atoms and the spectral distribution of fluorescent radiation from the excited-state atoms are assumed to be constant and nonzero over a narrow range of frequencies which is common to both.

The modified diffusion equation as first derived by Milne[13,17] may be written

$$\nabla^2 \left(n^* + \tau \frac{\partial n^*}{\partial t}\right) = 4k^2\tau \frac{\partial n^*}{\partial t} \tag{1}$$

where (i) ∇^2 is the Laplacian in a coordinate system appropriate to the experimental cell geometry, (ii) τ is the natural radiative lifetime of the excited state, and (iii) k is the absorption coefficient (in cm^{-1}) and is directly proportional to n. The dimensionless product of k and an appropriate length characteristic of the vessel is often called the "opacity" or "optical depth" of the system.

Equation 1 can be solved easily for three geometries which may be useful approximations to common experimental cell configurations.

Infinite Slab Geometry. If the external radiation source is turned off at $t = 0$, there is zero inward radiation flux (I^-) at the cell boundary for times $t > 0$. As shown by Milne this boundary condition, when applied to an infinite slab of thickness l, may be expressed as follows:

$$I^-(x = l) \propto \left(n^* + \tau \frac{\partial n^*}{\partial t}\right) + \frac{1}{2k}\frac{\partial}{\partial x}\left(n^* + \tau \frac{\partial n^*}{\partial t}\right) = 0 \tag{2}$$

After solving eq 1 in rectangular coordinates (which are appropriate to the slab geometry) and then applying the boundary condition (eq 2), one finds for the ratio of the so-called "imprisoned" lifetime τ_1 to the natural lifetime τ:

$$\tau_1/\tau = 1 + (kl/y_1)^2 \tag{3}$$

where y_1 is the first root of

$$\tan y = kl/y \tag{4}$$

The excited state decay is actually described by a series of exponential terms e^{-t/τ_m} including all possible roots of eq 4, where τ_m is the decay time of the mth mode corresponding to the mth root. It is customary to retain only the first term e^{-t/τ_1}, although, as we show later, higher terms may contribute significantly at short times following the initial cutoff of the external radiation source.

Infinite Cylinder Geometry. To solve eq 1 for an infinite cylinder of radius R under conditions of uniform external radiation, the angular and axial terms of the Laplacian may be ignored since these coordinates will not contribute to net decay. Equation 1 thus may be written

$$\frac{1}{r}\frac{\partial}{\partial r}\left(r\frac{\partial}{\partial r}\right)\left(n^* + \tau \frac{\partial n^*}{\partial t}\right) = 4k^2\tau \frac{\partial n^*}{\partial t} \tag{5}$$

The associated boundary condition expressing the absence of inward light flux for $t > 0$ is

$$I^-(r = R) \propto \left(n^* + \tau \frac{\partial n^*}{\partial t}\right) + \frac{1}{2k}\frac{\partial}{\partial r}\left(n^* + \tau \frac{\partial n^*}{\partial t}\right) = 0 \tag{6}$$

If we assume that $n(r,t) = F(r)\cdot g(t)$, the variables may be readily separated to give

$$\frac{d^2F}{dr^2} + \frac{1}{r}\frac{dF}{dr} + \lambda^2 F = 0 \tag{7}$$

and

$$(\lambda^2 + 4k^2)\tau \frac{dg}{dt} + \lambda^2 g = 0 \tag{8}$$

where λ^2 is the separation constant. λ may be eliminated from the radial eq 7 by substituting $x = \lambda r$:

$$\frac{d^2F}{dx^2} + \frac{1}{x}\frac{dF}{dx} + F = 0$$

The solution of this equation is the zero-order Bessel function $J_0(x)$. The time dependence of n^* is obtained from the solution of eq 8

$$g(t) = \exp\left[-\left(\frac{\lambda^2}{\lambda^2 + 4k^2}\right)\frac{t}{\tau}\right]$$

The boundary condition (eq 6) restricts λ to values satisfying

$$\lambda_m R\, J_1(\lambda_m R) - 2kR\, J_0(\lambda_m R) = 0 \tag{9}$$

which follows directly upon substituting the general solution

$$n^*(r,t) = \sum_{m=1}^{\infty} A_m\, J_0(\lambda_m r) e^{-t/\tau_m} \tag{10}$$

into eq 6 and making use of the relation $J_0'(x) = -J_1(x)$. The decay times τ_m in the expansion are given by

$$\tau_m = \tau\left(1 + 4\frac{k^2}{{\lambda_m}^2}\right) = \tau\left[1 + 4\left(\frac{kR}{x_m}\right)^2\right] \tag{11}$$

where $x_m = \lambda_m R$ is the mth root of $x\, J_1(x) - 2kR J_0(x) = 0$.[20] The amplitudes $\{A_m\}$ are determined by the distribution of excited atoms in the cell at $t = 0$ (see Appendix).

As in the case of infinite slab geometry, a series of decay modes is obtained (see Appendix). For low opacities the first decay mode e^{-t/τ_1} will describe the decay adequately for times sufficiently long after cutoff. The lifetime τ_1 may be calculated for different opacities using eq 11 with $m = 1$. Figure 1 presents curves (solid lines) of τ_1/τ vs. opacity (kl or kR) for infinite slab and infinite cylinder geometry.

The near equivalence at low opacities of an infinite cylinder with radius R to an infinite slab with thickness $l = R$ is striking and provides theoretical justification for the observations of Michael and Yeh,[8] and for the imprisonment treatment used by Breckenridge and coworkers.[3]

Spherical Geometry. To solve eq 1 for a spherical vessel, angular terms in the spherical Laplacian may be neglected, so that eq 1 assumes the form

$$\frac{1}{r^2}\frac{\partial}{\partial r}\left(r^2\frac{\partial}{\partial r}\right)\left(n^* + \tau \frac{\partial n^*}{\partial t}\right) = 4k^2\tau \frac{\partial n^*}{\partial t}$$

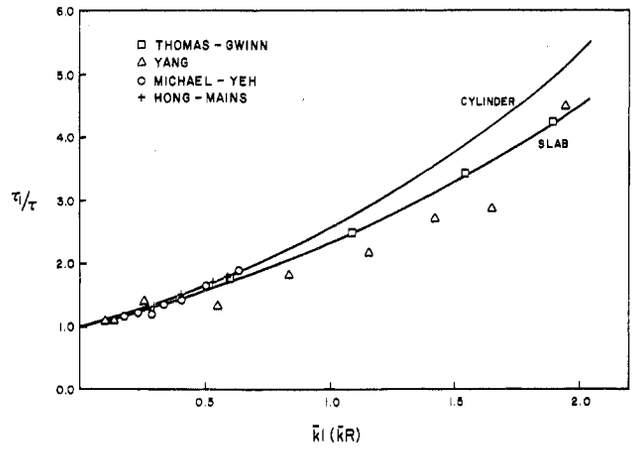

Figure 1. Plots (solid lines) of the "imprisonment" lifetime τ_1 relative to the natural lifetime τ, as a function of equivalent opacity $\bar{k}l$ ($\bar{k}R$) for infinite slab and infinite cylinder vessel geometry. (See text.) Data points are experimental measurements of $Hg(^3P_1)$ lifetimes (see text for explanation): (□) ref 21; (△) ref 9; (○) ref 8; (+) ref 10.

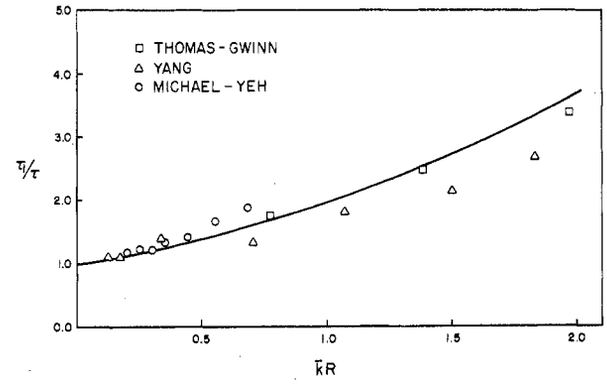

Figure 2. Plots (solid lines) of the "imprisonment" lifetime τ_1 relative to the natural lifetime τ, as a function of equivalent opacity $\bar{k}R$ for spherical vessel geometry. (See text.) Data points are experimental measurements of $Hg(^3P_1)$ lifetimes (see text for explanation): (□) ref 21; (△) ref 9; (○) ref 8.

Separation of variables ($n^*(r,t) = G(r)\cdot f(t)$) leads to a radial equation

$$\frac{d^2G}{dr^2} + \frac{2}{r}\frac{dG}{dr} + \lambda^2 G = 0 \qquad (12)$$

The associated time equation is identical with eq 8 obtained for an infinite cylinder. Equation 12 may be solved by first making the substitution $u(r) = r^{1/2}G(r)$. After some rearrangement the following equation is obtained:

$$\frac{d^2u}{dr^2} + \frac{1}{r}\frac{du}{dr} + \left(\lambda^2 - \frac{1/4}{r^2}\right)u = 0$$

with $x = \lambda r$ this simplifies to

$$x^2\frac{d^2u}{dx^2} + x\frac{du}{dx} + (x^2 - 1/4)u = 0$$

which is the differential equation obeyed by the half-integer Bessel function $J_{1/2}(x)$. Thus $u(r) = J_{1/2}(\lambda r)$ and $G(r) = r^{-1/2}u(r) = r^{-1/2}J_{1/2}(\lambda r) \equiv j_0(\lambda r)$, where j_0 is the zero-order spherical Bessel function. The general solution is therefore $n^*(r,t) = \Sigma_{m=1}^{\infty} A_m\, j_0(\lambda_m r)e^{-t/\tau_m}$ which is identical in form with eq 10 for an infinite cylinder.

The condition of zero inward radiation flux on the surface ($r = R$) of the sphere leads to the equivalent of eq 9 with J_1 and J_0 replaced by j_1 and j_0, respectively. The first zero of this modification of eq 9 was found by means of a Newton–Raphson iteration routine and then used in eq 11 to calculate imprisonment factors τ_1/τ for spherical geometry (shown in Figure 2, solid line).

Selected values of τ_1/τ for infinite slab, infinite cylinder, and sphere are given in Table I.

The Approach to Steady State. Experimental measurements are often made under "steady-state" conditions, where the rate of formation of excited state atoms by absorption of external resonance radiation is equal to the rate of disappearance of the excited atoms (via fluorescence or collisional quenching). In this section we investigate the effect of radiation imprisonment on the approach to the steady state when the external source of radiation is turned on at $t = 0$. We treat, as an example, the case of an infinite cylindrical vessel irradiated with a surrounding coaxial light source. The basic rate equation is

TABLE I: Calculated Imprisonment Lifetimes τ_1/τ as a Function of Opacity For Different Vessel Geometries

	τ_1/τ		
Opacity (kl or kR)	Infinite slab	Infinite cylinder	Sphere
0.1	1.103	1.105	1.069
0.2	1.214	1.220	1.144
0.3	1.331	1.347	1.225
0.4	1.458	1.485	1.312
0.5	1.586	1.634	1.405
0.6	1.725	1.790	1.505
0.7	1.870	1.962	1.612
0.8	2.020	2.153	1.725
0.9	2.183	2.343	1.845
1.0	2.355	2.562	1.972
1.1	2.526	2.774	2.106
1.2	2.708	3.017	2.249
1.3	2.898	3.265	2.397
1.4	3.096	3.502	2.554
1.5	3.304	3.775	2.718
1.6	3.519	4.058	2.890
1.7	3.737	4.353	3.070
1.8	3.966	4.667	3.257
1.9	4.201	4.998	3.452
2.0	4.470	5.340	3.655

$$dn^*/dt = K - \beta n^* - k_Q[Q]n^* \qquad (13)$$

where (i) K is the rate of absorption of external radiation (in photons per second per unit volume), and of course is a function of n; (ii) k_Q is the bimolecular rate constant for the quenching of n^* by an added gas Q; (iii) [Q] is the concentration of Q; (iv) β is a composite of the decay modes discussed above and in the Appendix, and may be found by taking the first time derivative of n^* (i.e., as given in eq 10):

$$\beta = \frac{\sum(A_m/\tau_m)\, J_0(\lambda_m r)e^{-t/\tau_m}}{n^*} \qquad (14)$$

In the limit of very long times ($t > 10\tau$), β reduces to $1/\tau_1$ and single mode behavior will be observed.

The lifetimes τ_m found in the previous section for a pulsed decay experiment are equally valid in the description of a steady-state experiment. Due to the cylindrical symmetry of the cell and the surrounding coaxial source, the distribution of excited atoms within the cell is symmetric for all times t. This is in marked contrast to the infinite

slab case when only one side is illuminated. As shown by Van Volkenburgh and Carrington[5] the resulting asymmetric distribution of excited atoms gives rise to imprisonment factors which not only depend on viewing location but also are different for pulsed and steady-state experiments.

The approach to steady state is therefore provided by the solution of eq 13

$$n^* = \frac{K}{(\beta + k_Q[Q])}\left[1 - e^{-t(\beta + k_Q[Q])}\right] \tag{15}$$

For short times ($t < \tau$, also depending on the opacity; see Appendix), the rise of n^* is not a true exponential, since β itself is a function of t. For times sufficiently long that the first mode predominates:

$$n^* = \frac{K}{(1/\tau_1 + k_Q[Q])}\left[1 - e^{-t((1/\tau_1) + k_Q[Q])}\right]$$

indicating true exponential behavior. When $t = \infty$ (the steady state):

$$\frac{K}{n^*} = \frac{1}{\tau_1} + k_Q[Q] \tag{16}$$

which is of the familiar Stern–Volmer form. Thus Stern–Volmer quenching measurements at low opacity can be corrected for radiation imprisonment simply by substituting the lowest mode lifetime τ_1 for the natural lifetime τ.

In addition to the surrounding coaxial light source, two other common experimental arrangements need to be considered: (1) excitation from a source placed at one end of a long cylindrical cell. In this case the distribution will be axially symmetric if the excitation beam is coaxial with the cell. Hence eq 14 and 15 are valid; (2) excitation lamp placed alongside the cell and parallel to it. This clearly leads to an asymmetric distribution. A special solution of eq 12 for this case is required and will lead to a new set of decay times τ_m.

III. The Use of Equivalent Opacity in the Diffusion Model

The idealized "step-function" atomic absorption and emission line shape adopted in the previous section is of course not observed in nature. For the usual situation at low total pressures, for example, the line-shape spectral function is determined by Doppler broadening[13] and is Gaussian:

$$k_\nu/k_0 = F(\omega) = e^{-\omega^2} \tag{17}$$

where k_ν is the absorption coefficient at any frequency ν; k_0 is the absorption coefficient at the Doppler line center:

$$k_0 = \frac{(\ln 2)^{1/2}\,\lambda_0^2\,g_2 n}{4(\Delta\nu_D)\pi^{3/2}\,g_1\tau}$$

where g_2 and g_1 are the statistical weights of the upper and lower states, respectively, λ_0 is the wavelength at the center of the atomic line, and

$$\Delta\nu_D = \left(\frac{2\nu_0}{c}\right)\left(\frac{2RT\ln 2}{M}\right)^{1/2}$$

where c is the velocity of light, R is the gas constant, T is the absolute temperature, and M the atomic weight; and ω is a convenient frequency variable defined in terms of the Doppler breadth:

$$\omega = \left[\frac{2(\nu - \nu_0)}{\Delta\nu_D}\right](\ln 2)^{1/2}$$

To utilize the simple diffusion model, an "equivalent" opacity $\bar{k}l$ is defined which an idealized atomic gas must have in order for resonance radiation to be propagated in the same way as the actual Doppler radiation under real conditions. The equivalent opacity for a generalized line shape $F(\omega)$ is given by:[3,13,18]

$$e^{-\bar{k}l} = \frac{\int_{-\infty}^{+\infty} F(\omega)\exp[-k_0 l\,F(\omega)]\,d\omega}{\int_{-\infty}^{+\infty} F(\omega)\,d\omega} \tag{18}$$

The right-hand side of eq 18 merely describes the transmission of incoherently scattered atomic radiation with line shape $F(\omega)$; the probability of light absorption is proportional to $F(\omega)$, but the intensity of the scattered light also follows an $F(\omega)$ spectral distribution.

The original criticism of Holstein[6] that the use of such an "equivalent" opacity $\bar{k}l$ is incorrect is based on the *valid* contention that any diffusion theory of radiation imprisonment assumes that the probability of a photon penetrating a certain distance in the atomic gas is given by a single exponential expression, which is true strictly speaking only if the absorption coefficient of the gas varies little over the frequency spectrum of the resonance quantum. That is never exactly true, of course, and Holstein proved that because it is therefore impossible to apply the concept of mean free path of resonance-radiation quanta, any simple kinetic theory of radiation diffusion is bound to be incorrect.

Doppler Line Shape. We accept Holstein's argument and agree that at high opacities the use of a simple equivalent opacity is entirely incorrect, leading to the failure of the diffusion model.[6,8] However, it can be shown that at *low* opacities the propagation of a Doppler-broadened line can be described adequately by a single exponential function, so that the concept of a photon mean free path leads to negligible error and diffusion theory expressions are consequently meaningful. Yang[9] has shown, for example, by numerical integration that for opacities ($k_0 l$) up to 1.00, the probability $P(l)$ that a Doppler photon will travel a distance l can be given accurately (less than 2% error) by the expression: $\exp(-0.675k_0 l)$ (i.e., an equivalent opacity $\bar{k}l = 0.675k_0 l$ is strictly valid up to $k_0 l = 1.00$). Only at much higher opacities, then, will the assumption of a photon mean free path invalidate the diffusion treatment for the Doppler line shape. Values of $\bar{k}l$ for the Doppler case, obtained by interpolation of values obtained by Zemansky by graphical integration,[13] are shown in Table II.

The only extensive low-opacity imprisonment measurements with which to test the diffusion theory are those for $Hg(^3P_1)$ under Doppler conditions.[8-10,21] In the $Hg(^3P_1)$ case, the resonance line is actually split into five separate Doppler-broadened hyperfine and isotopic components, which to a good approximation can be taken to be equal in intensity.[22] Thus the diffusion theory can be applied by simply assuming that the imprisonment would be equivalent to that of a single line with maximum absorption coefficient $k_0/5$.[13] The reaction vessels used in experimental studies, which are usually cylindrical, are rarely good approximations to the theoretical geometries treated in the previous section, so that the experimental points in Figures 1 and 2 were plotted in the following manner. For a given experimental determination of τ_1/τ, $k_0/5$ was calculated from the known mercury vapor concentration. The characteristic length needed to obtain the opacity was taken as

TABLE II: Equivalent Opacity $\bar{k}l$ as a Function of Opacity k_0l for a Doppler-Broadened Atomic Line

k_0l	$\bar{k}l$	$\bar{k}l/k_0l$
0.00	0.00	0.675
1.00	0.665	0.665
1.50	0.965	0.643
2.00	1.241	0.621
2.50	1.49	0.597
3.00	1.72	0.572
3.50	1.92	0.549
4.00	2.10	0.526

follows.[23] (i) The thickness l of the hypothetical infinite slab or the radius R of the hypothetical infinite cylinder was set equal to the radius of the experimental vessel. (ii) The diameter of the hypothetical sphere was set equal to the average of the diameter and the length of the experimental vessel. The equivalent opacity $\bar{k}l$ was then obtained from Table II. It is obvious that no matter which geometric approximation is used, the diffusion model predicts both the onset of imprisonment and the form of the τ_1/τ curve at effective opacities (k_0l) less than 1.0 ($\bar{k}l < 0.7$) for Doppler-broadening conditions. Approximating the experimental vessels as spheres seems to give the best fit of all the available data, but more experimental measurements in the $1.0 < \bar{k}l < 2.0$ region are required to test the theory adequately.

Further proof that the diffusion theory is valid in the low-opacity region can be obtained by comparing the exact calculations of Van Volkenburgh and Carrington[24] for the one-dimensional infinite slab Doppler-broadening case with the imprisonment lifetime predictions of the diffusion theory (as shown in the first column in Table I).

Since tabulated values of τ_1/τ were not given in ref 24, estimates were read from the plots, yielding satisfactory agreement with the predictions of the diffusion theory (Tables I and II) for opacities k_0l up to 3.0.

Lorentz Line Shape. It is useful to extend the concept of equivalent opacity to other commonly encountered absorption line shapes. At very high total pressures, the absorption profile is dictated almost entirely by the perturbing collisions of the absorbing or emitting atoms with each other or with a "bath" gas (i.e., Holtsmark or Lorentz broadening). In these cases the line-shape function can be expressed as

$$F(\omega) = \frac{k_{max}}{k_0}\left(\frac{1}{1+y^2}\right) \tag{19}$$

where k_{max} is the maximum absorption coefficient (at the center of the Lorentz line), $y = \omega/a$, $a = (\Delta\nu_L/\Delta\nu_D)(\ln 2)^{1/2}$, and $\Delta\nu_L$ is the Lorentz breadth (which is given in simplest form as Z_L/π, where Z_L is the effective number of broadening collisions per second per absorbing atom).[13] Note that $k_{max} = k_0/\pi^{1/2}a$.[13] In the Lorentzian case, the right side of eq 18 can be integrated exactly to yield:

$$\exp\left[-\left(\frac{k_{max}l}{2}\right)\right] I_0\left(\frac{k_{max}l}{2}\right)$$

where $I_0(k_{max}l/2)$ is the modified Bessel function of order zero. Values of $\bar{k}l$ for various values of $k_{max}l$ are given in Table III.

Although $\bar{k}l$ is not a strictly linear function of $k_{max}l$ even at low $k_{max}l$, use of $\bar{k}l$ at values of $k_{max}l \leq 2$ should not lead to significant error.

Also, for a given atomic vapor concentration, k_{max}/k_0 will be less than ~0.05 for the line to be accurately described as a Lorentz-broadened line, with no contribution from Doppler broadening[13] (i.e., because of the severe broadening of the line, the maximum absorption coefficient k_{max} will be much less than the maximum absorption coefficient under Doppler-only conditions, k_0). Radiation imprisonment is therefore much less severe under Lorentz broadening conditions.

TABLE III: Equivalent Opacity $\bar{k}l$ as a Function of $k_{max}l$ for a Lorentz-Broadened Atomic Line

$k_{max}l$	$\bar{k}l$	$\bar{k}l/k_{max}l$
0.0	0.000	0.500
0.2	0.098	0.488
0.4	0.190	0.475
0.6	0.278	0.463
0.8	0.360	0.450
1.0	0.439	0.439
1.2	0.512	0.427
1.4	0.581	0.415
1.6	0.651	0.407
1.8	0.707	0.393
2.0	0.764	0.382

Voigt Line Shape. Unfortunately, it is often convenient to conduct experiments with a buffer gas present at pressures greater than 1 Torr but less than several atmospheres, in which case the line shape is influenced by Doppler, Lorentz, and sometimes natural (Heisenberg) broadening.[13,25] The line shape functional dependence, $F(\omega)$ (often called the Voigt profile), will therefore vary with the total pressure of buffer gas:

$$F(\omega) = \frac{a'}{\pi}\int_{-\infty}^{+\infty}\frac{e^{-z^2}\,dz}{(a')^2 + (\omega - z)^2} \tag{20}$$

where $z = (2\zeta/\Delta\nu_D)(\ln 2)^{1/2}$, and ζ is the frequency variable for integration in this equation (i.e., $\omega - z = [2(\ln 2)^{1/2}/\Delta\nu_D](\nu - \nu_0 - \zeta)$); $a' = [(\Delta\nu_L + \Delta\nu_N)/\Delta\nu_D](\ln 2)^{1/2}$, where $\Delta\nu_N$ is the natural linewidth and can be expressed as $1/2\pi\tau$. Equation 20 can be understood as the summation of all the Doppler-broadened infinitesimal components of a pure (Lorentz + natural)-broadened line.

Values of $F(\omega)$ for appropriate values of ω for $a' = 0.5$, 1.0, 1.5, and 2.0 have been determined by Zemansky by a series expansion and are found in the Appendix of ref 13. Using these values, approximate determinations of the right-hand side of eq 18 have been made for $a' = 0.5$, 1.0, 1.5, and 2.0 by replacing the integrals with summations. The values of the equivalent opacities $\bar{k}l$ thereby calculated are given in Table IV. To obtain an indication of the accuracy of the summation approximation, we have also determined equivalent opacities for $a' = 0$, which is identical with a purely Doppler line shape, and included these values in Table IV. Summation intervals were chosen to be comparable to those used for $a' = 0.5$–2.0. Comparison with the more accurate determinations in Table II shows that the summation approximation is a good one with an error of less than 3%.

Values of a' greater than 2.0 will rarely be encountered in laboratory work. Even for the $^3P_1$ state of the heavy atom mercury, $a' = 2.0$ corresponds roughly to the line shape in 300 Torr of Ar at room temperature. For lighter atoms, $a' = 2.0$ would describe experimental situations nearer 1 atm of buffer gas.

Complications Due to Hyperfine and Isotope Splitting. For atomic transitions where the line shape is affected by isotopic and/or hyperfine splitting, there may be compli-

TABLE IV: Equivalent Opacity $\bar{k}l$ as a Function of Opacity k_0l for a Voigt-Profile Atomic Line at Different Values of a' (See Text)

	k_0l	$\bar{k}l$	$\bar{k}l/k_{max}l$
	$a' = 0.00$		
$(k_{max}l = k_0l)$	1.0	0.683	0.683
	2.0	1.273	0.636
	3.0	1.764	0.588
	4.0	2.161	0.540
	$a' = 0.50$		
$(k_{max}l = 0.615k_0l)$	0.25	0.104	0.674
	0.50	0.205	0.666
	0.75	0.304	0.658
	1.00	0.400	0.650
	2.00	0.758	0.616
	3.00	1.07	0.580
	4.00	1.34	0.544
	5.00	1.57	0.509
	$a' = 1.00$		
$(k_{max}l = 0.428k_0l)$	0.25	0.0664	0.621
	0.50	0.132	0.615
	0.75	0.195	0.609
	1.00	0.258	0.603
	2.00	0.495	0.579
	3.00	0.710	0.554
	4.00	0.905	0.529
	5.00	1.08	0.504
	6.00	1.23	0.481
	$a' = 1.50$		
$(k_{max}l = 0.322k_0l)$	0.25	0.0508	0.632
	0.50	0.101	0.627
	0.75	0.150	0.622
	1.00	0.199	0.617
	2.00	0.384	0.597
	3.00	0.556	0.576
	4.00	0.714	0.555
	5.00	0.859	0.534
	6.00	0.990	0.513
	7.00	1.11	0.493
	$a' = 2.00$		
$(k_{max}l = 0.256k_0l)$	0.50	0.0817	0.638
	1.00	0.162	0.632
	2.00	0.316	0.618
	4.00	0.605	0.591
	6.00	0.866	0.564
	8.00	1.10	0.537
	10.00	1.31	0.511
	12.00	1.50	0.487

cated and irregular line shapes, especially under Voigt profile conditions. In such cases, $F(\omega)$ may have to be determined graphically by summation of each spectral component, and eq 18 must then be integrated graphically.[3,13]

IV. Use of the Diffusion Model

It is instructive to summarize here the procedure for the use of the low-opacity diffusion model in a particular experimental situation. From the atom concentration n, the maximum absorption coefficient k_0 for Doppler conditions may be calculated using the expression following eq 17. The theoretical geometry (infinite slab, infinite cylinder, or sphere) which best approximates the experimental vessel is adopted, a characteristic length l (or R) is chosen, and the opacity k_0l (or k_0R) calculated.

The equivalent opacity $\bar{k}l$ ($\bar{k}R$) is determined as follows. (i) If the line shape can be represented as pure Doppler broadening of a single component, $\bar{k}l$ ($\bar{k}R$) can be found using Table II. (ii) For a pure Lorentz-broadened single line, k_{max} ($= k_0/\pi^{1/2}a$) is calculated (see following eq 19 for definition of the quantity (a)), and $\bar{k}l$ ($\bar{k}R$) is obtained using Table III. (iii) For a single line with a Voigt profile, a' is calculated (see following eq 20 for definition), and $\bar{k}l$ is determined using Table IV (by interpolation between given values of a'). (iv) For atomic lines with hyperfine and/or isotopic structure, $F(\omega)$ must be estimated graphically by direct summation of the line shape of each component (for the applicable broadening conditions). The equivalent opacity $\bar{k}l$ ($\bar{k}R$) must then be calculated by graphical integration of eq 18.

Finally, when $\bar{k}l$ ($\bar{k}R$) has been determined for the particular atomic line and experimental conditions of interest, τ_1/τ can be obtained directly from Table I.

Acknowledgments. Acknowledgment is made to the donors of the Petroleum Research Fund, administered by the American Chemical Society, for partial support of this research. Acknowledgment of financial assistance is also made to the National Science Foundation (Grant No. MPS-12851).

The authors wish to thank Drs. Frank Stenger and Robert Rubinstein of the Department of Mathematics, University of Utah, for assistance in integrating eq 18 for the Lorentzian case.

Appendix

The amplitudes $\{A_m\}$ of eq 10 are determined by the initial distribution within the cylindrical geometry

$$n^*(r;t = 0) = \sum_{m=1}^{\infty} A_m J_0(\lambda_m r) \quad \text{(I)}$$

which is assumed to be axially symmetric and of the form

$$f(r) = e^{-k(R+r)} + e^{-k(R-r)} \quad \text{(II)}$$

simulating the effect of a surrounding coaxial source.

In our numerical studies, series I was arbitrarily truncated at five terms. By means of standard least-squares and matrix inversion techniques the five coefficients (A_1, ···, A_5) were adjusted to give the best fit of the functions ($J_0(\lambda_1 r)$, ···, $J_0(\lambda_5 r)$) to the distribution $f(r)$ at 10 equally spaced points ranging from the center of the cylinder to the wall. The results for different opacities are summarized in Table V. The agreement between the calculated distribution $\Sigma_{m=1}^{5} A_m J_0(\lambda_m r)$ and the assumed distribution (eq II) was excellent for the lowest opacity and fair for the highest opacity ($kR = 2.0$) employed in the calculations.

As indicated in eq 10 the time behavior of the excited atoms after cutoff is given by a series of exponential terms e^{-t/τ_m} each with a weighting factor $A_m J_0(\lambda_m r)$. It is interesting to inquire under what conditions the decay may be adequately described by a single decay mode. Table VI gives the first five terms of the expansion for selected opacities $kR = 0.2$, 1.0, and 2.0 and for times ranging from 0.1 to 10.0 (in units of the natural decay time τ). The terms are evaluated at the center ($r = 0$) of the reaction vessel where $J_0(\lambda_m r) = 1.0$ for each m. We adopt an arbitrary definition of single mode behavior when the first term is at least a factor of 10 greater in magnitude than the largest of the remaining terms (i.e., $|A_1 e^{-t/\tau_1}| \geq 10|A_m e^{-t/\tau_m}|$). Thus we see that for $t = 0.1\tau$, this criterion is not satisfied for any opacity in the range 0–2.0, and one or more of the higher terms will contribute significantly to the radiation decay. When $t = \tau$ single-mode behavior will be observed when the opacity $kR < 1.0$. When $t = 10\tau$, single mode behavior is found throughout the range $kR = 0$–2.0. For any given

TABLE V: Expansion Coefficients for an Infinite Cylinder ($A_1 = 1.00$)

kR	A_2	A_3	A_4	A_5
0.2	−0.117	0.039	−0.015	0.004
0.4	0.074	−0.144	0.077	−0.052
0.6	−0.151	0.020	−0.018	−0.007
0.8	−0.066	−0.161	0.129	−0.081
1.0	−0.252	0.008	−0.008	−0.016
1.2	−0.195	−0.161	0.168	−0.115
1.4	−0.369	0.009	0.012	−0.033
1.6	−0.327	−0.149	0.202	−0.149
1.8	−0.490	0.024	0.032	−0.054
2.0	−0.452	−0.129	0.230	−0.178

TABLE VI: Mode Structure for Infinite Cylinder ($A_1 e^{-t/\tau_1} = 1.00$)

	t/τ	$\lvert A_2 e^{-t/\tau_2}\rvert$	$\lvert A_3 e^{-t/\tau_3}\rvert$	$\lvert A_4 e^{-t/\tau_4}\rvert$	$\lvert A_5 e^{-t/\tau_5}\rvert$
$kR = 0.2$	0.1	0.115	0.038	0.014	0.004
	1.0	0.099	0.032	0.012	0.003
	10.0	0.021	0.007	0.002	0.001
$kR = 1.0$	0.1	0.242	0.008	0.008	0.015
	1.0	0.164	0.005	0.005	0.009
	10.0	0.003	0.000	0.000	0.000
$kR = 2.0$	0.1	0.435	0.122	0.215	0.166
	1.0	0.307	0.071	0.116	0.086
	10.0	0.010	0.000	0.000	0.000

opacity the relative importance of the lowest mode increases with time, since the higher modes decay more rapidly.

References and Notes

(1) Dreyfus Foundation Teacher-Scholar.
(2) Alfred P. Sloan Fellow.
(3) W. H. Breckenridge, T. M. Broadbent, and D. S. Moore, *J. Phys. Chem.*, **79**, 1233 (1975).
(4) R. J. Cvetanović, *Prog. React. Kinet.*, **2**, 39 (1964).
(5) G. V. Van Volkenburgh and T. Carrington, *J. Quant. Spectrosc. Radiat. Transfer*, **11**, 1181 (1971).
(6) T. Holstein, *Phys. Rev.*, **72**, 1212 (1947).
(7) T. Holstein, *Phys. Rev.*, **83**, 1159 (1951).
(8) J. V. Michael and C. Yeh, *J. Chem. Phys.*, **53**, 59 (1970).
(9) K. Yang, *J. Am. Chem. Soc.*, **88**, 4575 (1966).
(10) J. Hong and G. J. Mains, *J. Photochem.*, **1**, 463 (1972–1973).
(11) A. J. Yarwood, O. P. Strausz, and H. E. Gunning, *J. Chem. Phys.*, **41**, 1705 (1964).
(12) L. F. Phillips, *J. Photochem.*, **2**, 255 (1973–1974).
(13) A. C. G. Mitchell and M. W. Zemansky, "Resonance Radiation and Excited Atoms", Cambridge University Press, London, 1971.
(14) W. H. Breckenridge and T. W. Broadbent, *Chem. Phys. Lett.*, **29**, 421 (1974).
(15) The "opacity" of an absorbing system is conventionally defined as the product of the maximum absorption coefficient, k_0, at the line center when Doppler broadening alone is present, and some characteristic length, l, of the vessel geometry (e.g., the radius of an infinite cylinder). The magnitude of k_0 is obviously directly proportional to the concentration of ground-state atoms.
(16) P. Alpert, A. O. McCoubrey, and T. Holstein, *Phys. Rev.*, **76**, 1257 (1949).
(17) E. A. Milne, *J. London Math. Soc.*, **1**, 40 (1926).
(18) E. W. Samson, *Phys. Rev.*, **40**, 940 (1932).
(19) L. M. Biberman, *Zh. Eksp. Teor. Fiz.*, **17**, 416 (1947).
(20) M. Abramowitz and I. A. Stegun, "Handbook of Mathematical Functions", Dover Publications, New York, N.Y., 1965.
(21) L. B. Thomas and W. D. Gwinn, *J. Am. Chem. Soc.*, **70**, 2643 (1948).
(22) R. Wallenstein and T. W. Hänsch, *Opt. Commun.*, **14**, 353 (1975).
(23) The characteristic length for the irregular vessel in the Hong-Mains study was taken to be their quoted value of 2.31 cm in all cases.
(24) See Figures 7 and 8 in ref 5.
(25) P. J. Walsh, *Phys. Rev.*, **116**, 511 (1959).

On the Stereochemistry of the Bromine for Chlorine Exchange following $^{79}Br(n,\gamma)^{80m}Br$ and $^{82m(80m)}Br(IT)^{82(80)}Br$ in Diastereomeric 2,3-Dichlorobutanes[1]

Ying-yet Su and Hans J. Ache*

Department of Chemistry, Virginia Polytechnic Institute and State University, Blacksburg, Virginia 24061

(Received August 11, 1975)

The stereochemistry of bromine for chlorine substitution at asymmetric carbon atoms was studied in the pure liquid diastereomeric 2,3-dichlorobutanes and in organic solutions of these compounds. The reactive bromine species were either energetic (hot) ^{80m}Br atoms generated via the $^{79}Br(n,\gamma)^{80m}Br$ nuclear process or bromine species formed as a result of Coulomb fragmentation of ^{80m}Br- or ^{82m}Br-labeled molecules. Distinct differences in the stereospecificity of the Br for Cl exchange have been observed depending on the type of nuclear process by which the reactive bromine species are formed and on the amount and nature of the additives present. In the case of the decay induced ^{80}Br for Cl exchange the observed results can be explained in terms of a model in which the neutralization time for the Br^+ and the time for radical recombination are the determining factors for the stereochemical course of the exchange process. The Br for Cl exchange initiated by "hot" ^{80m}Br atoms appears to be primarily the result of a "hot" one-step replacement reaction, as indicated by the presence of a strong conformational effect on the stereochemical course of the reaction.

Introduction

The reactions of radiobromine generated by nuclear processes, such as the radiative neutron capture (n,γ) or the isomeric transition activation process, have been the subject of a large number of investigations.[2]

One of the major objectives in these studies was to assess the effect of the type of the nuclear reaction by which the radiobromine is generated on the final product spectrum of radiobromine labeled compounds.

Earlier work stressed the similarity of the chemical prod-